A FINITE VOLUME MODEL FOR THE HOT ROLLING PROCESS[1]

Jose Adilson de Castro [2]
Luciano Pessanha Moreira [2]

Abstract

A finite volume model for the hot rolling process is proposed to determine useful parameters in the hot rolling process such as the loads, temperature, stress and strain fields and the microstructure evolution. A non-newtonian formulation and Eulerian description are adopted with the finite volume method. The strain-rate field is firstly obtained from the pressure and velocities solutions. Then, the temperature field together with a constitutive equation provides the apparent viscosity of the material and thus the stress field. The adopted constitutive equations describe the microstructural phenomena occurring in the hot rolling, i.e., work-hardening, recovery and recrystallisation. The predictions obtained with the proposed finite volume model are in good agreement with the industrial measured rolling loads and surface temperatures for the 7-stand finishing mill of a C-Mn steel strip

Key-words: Hot rolling; Modeling; Finite volume; Microstructure; Heat transfer.

UM MODELO DE VOLUMES FINITOS PARA O PROCESSO DE LAMINAÇÃO A QUENTE

Resumo

Um modelo de volumes finitos é proposto para determinar parâmetros úteis na laminação a quente tais como força de laminação, campos de temperatura, tensões e deformações e evolução microestrutural. Uma formulação Euleriana de fluido não Newtoniano é assumida usando o método de volumes finitos. Primeiramente o campo de taxa de deformação é obtido dos campos de velocidade e pressão. Em seguida o campo de temperaturas e com o auxilio de relações constitutivas a viscosidade aparente é determinada e então o campo de deformação é calculado. As relações constitutivas de evolução microestrutural considerando encruamento, recuperação e recristalização são utilizadas. As previsões do modelo estão em concordância com dados industriais de força de laminação e temperaturas de superfície para o trem acabador de 7 cadeiras de um aço C-Mn.

Palavras-chave: Laminação a quente; Modelagem; Volumes finitos; Microestrutura; Transferência de calor.

---

1 INTRODUCTION

The mathematical modeling of the hot rolling process is an extremely hard task because of the deformation coupled to the temperature, the microstructure phenomena as well as the range of temperatures, strains and strain-rates evolved which, in turn, cannot be well reproduced or even monitored under laboratory conditions. The mathematical models for describing the hot rolling process in the literature can vary from roll force and torque models based upon the works of Orowan[1] and Sims[2] up to integrated and stand alone Finite Element (FE) models, e.g., Zhou[3] and Mukhopadhyay et al.[4] In bulk metal forming processes such as the hot slab or strip rolling, the elastic strains are usually very small in comparison to the high plastic strain levels and then can be neglected. This assumption makes possible to consider the deformation process by means of a flow formulation together with the finite volume (FV) method. This approach is adopted in this work where the basic constitutive equations are first presented. Then, the transport equations are detailed for the 3D case in an Eulerian frame. The microstructural changes taking place during the hot rolling process are also taken into account with the flow-stress model used in the commercial software Slimmer.[5] The predictions forecasted with the proposed FV model are compared to the measured surface temperatures and rolling loads obtained from the hot strip rolling of a low C-Mn steel in an industrial 7-stand finishing mill.

2 MODELING

In bulk metal forming such as the hot rolling process, the final material properties depend essentially upon the strain, strain-rate and temperature fields. Considering firstly the assumption of small elastic strains, the total strain rate tensor can be split into an elastic part and a viscoplastic one:

$$\dot{\varepsilon}_{ij} = \dot{\varepsilon}_{ij}^{e} + \dot{\varepsilon}_{ij}^{vp} \tag{1}$$

Then, the elastic strains are usually very small in comparison to the plastic or viscoplastic strain levels in the hot rolling process and can, thus, be neglected. The total strain-rate is defined by the viscoplastic model of Perzyna:[6]

$$\dot{\varepsilon}_{ij}^{vp} = \gamma \left\langle \phi(F) \right\rangle \frac{\partial F}{\partial \sigma_{ij}} \tag{2}$$

In eq (2) γ is a fluidity parameter, σ_{ij} is the Cauchy stress tensor, where F is the von Mises yield function given by:

$$F = \sqrt{(3/2)S_{ij}S_{ij}} - \overline{\sigma} \tag{3}$$

in which $\overline{\sigma}$ is a scalar measure of the material flow-stress and S_{ij} is the deviatoric stress tensor. On the other hand, the behavior of a linear isotropic Newtonian fluid relates the deviatoric stress and the total or the viscoplastic strain-rate tensors through the viscosity that is,

$$S_{ij} = 2\mu\dot{\varepsilon}_{ij} \tag{4}$$

The strain-rates are obtained from the velocity field v_i in a Cartesian coordinate system x_i (i=1,2,3) by:

$$\dot{\varepsilon}_{ij} = \frac{1}{2}\left(\frac{\partial v_i}{\partial x_j} + \frac{\partial v_j}{\partial x_i}\right) \tag{5}$$

Afterwards by introducing firstly the definition of the effective strain-rate conjugated of the von Mises effective stress, Eq. (3),

$$\dot{\bar{\varepsilon}} = \sqrt{(2/3)\dot{\varepsilon}_{ij}\dot{\varepsilon}_{ij}} \tag{6}$$

and assuming $\gamma(F)$ as an exponential function $(F)^n$ and a viscoplastic loading stable condition of, $(F)^n > 0$, one obtains the viscosity from Eqs. (2-4) and (6):

$$\mu = \frac{\bar{\sigma}}{3\dot{\bar{\varepsilon}}} \tag{7}$$

The viscosity nonlinearity is accounted for through the flow stress definition which, in turn, depends upon the accumulated effective strains and strain-rates, the temperature and some internal variables defining the material microstructure. Thus, the material behaviour in bulk metal forming can be considered as rigid-viscoplastic likewise an incompressible non-Newtonian fluid. Furthermore, it should be noted that eq. (7) is only valid for a non-zero effective plastic strain-rate otherwise the material is a rigid body. For numerical purposes of stability, a small cut-off value is set equal to 0.01 s^{-1}. The material behaviour during the hot rolling process is highly coupled to the temperature and the strain-rate fields. Thus, the solution of the hot deformation is achieved by solving the temperature, velocity and pressure fields simultaneously. For a steady-state flow condition and assuming plastic strain incompressibility, the hot strip motion and temperature are obtained from the transport equations of conservation of energy, momentum and mass. These equations are described in an Eulerian or spatial reference frame. Firstly, the temperature T is calculated from the solution of the energy balance equation:

$$\rho C_p\left(v_i\frac{\partial T}{\partial x_j}\right) = \frac{\partial}{\partial x_j}\left(\frac{K}{C_p}\frac{\partial T}{\partial x_j}\right) + S_P + S_F \tag{8}$$

where ρ, C_p and K are the material density, specific heat per unit volume and conductivity respectively. The first source term S_P in eq. (7) is the rate of energy dissipation per unit volume resulting from the plastic deformation process:

$$S_P = (\eta/J)\int_V \sigma_{ij}\dot{\varepsilon}_{ij}\,dV \tag{9}$$

where η is the fraction of the plastic work which is transformed into heat and J is the mechanical equivalent of heat. The second source term S_F in Eq. (7) is the rate of energy dissipation due to the friction between the strip and the roll:

$$S_F = \int_S \tau \|\Delta v\| dS \qquad (10)$$

In eq (10) $\tau = f(\overline{\sigma}/\sqrt{3})$ is the shear stress at roll-strip interface where f is friction factor and $\|\Delta v\|$ is the norm of the velocity discontinuity.[7] Then, the velocity **v** and the pressure p are determined from the solution of the conservation of momentum given by:

$$\frac{\partial}{\partial x_j}(\rho v_j v_i) = \frac{\partial}{\partial x_j}\left(\mu \frac{\partial v_j}{\partial x_i}\right) - \frac{\partial p}{\partial x_i} \qquad (11)$$

Together with the conservation of mass or continuity equation:

$$\frac{\partial v_i}{\partial x_i} = 0 \qquad (12)$$

The transport equations are discretized using the finite volume method for the 3D case of an arbitrary domain, that is, a non-orthogonal domain, together with the "Body Fitted Coordinate" grid generation technique.[8]

The material behavior under hot deformation conditions is computed by determining constitutive laws. Figure 1 illustrates the typical flow-stress of low carbon steels deformed at high temperatures, where the mechanisms of work-hardening and restoration can be observed during the hot deformation process. The restoration events are respectively denoted as dynamic and static depending whether they take place concomitantly or not with the loading. At the onset of the deformation process, the material work hardens due to the increase of the density of dislocations, which are arranged into subgrains boundaries. As the plastic strain level rises, the annihilation and generation rates of dislocations are counteracted producing, consequently, a steady-state flow-stress shown by the plateau (a) in this figure. This restoration mechanism is known as dynamic recovery and its resulting microstructure, consisted of well-defined subgrains, is the source of the static recrystallisation nuclei. When the dynamic recovery is the only active restoration mechanism, the flow-stress can be described as presented at literature,[9] Eq.(13):

$$\sigma_e = \sigma_0 + (\sigma_{SS} - \sigma_0)\left[1 - \exp(-C\varepsilon)^m\right] \qquad (13)$$

where σ_0 is the flow-stress at zero plastic strain, σ_{ss} is the steady-state flow-stress and *m* is the work-hardening exponent. *C* depends upon the Zener-Hollomon parameter which is defined by $Z = \dot{\varepsilon}\exp[Q/(RT)]$, where *Q* is the apparent activation energy for deformation, *R* is the gas constant (8.31 J/K mol) and *T* is the absolute temperature of deformation. Likewise, the flow stresses σ_0 and σ_{ss} depend upon the deformation conditions and can be generally defined in the form of $\sigma_{FS} = A_1 \sinh^{-1}(Z/A_2)^{A3}$ where A_k are material parameters determined from experimental tests, such as hot plane-strain compression or torsion tests.

Moreover, when the recovery process is insufficient so as to decrease the activation energy of deformation, the multiplication of dislocations may produce the nucleation and growth of recrystallised grains during the hot deformation. In such a case, the flow-stress curve increases up to a maximum value, namely, the peak stress, accompanied by an additional softening reaching a steady-state value as shown by the plateau in curve (c), see Figure 1. The onset of dynamic recrystallisation is characterized by a critical strain which is estimated from the strain related to the peak in the flow-stress given by:

$$\varepsilon_p = A \, d_0^{\,p} \, Z^q \tag{14}$$

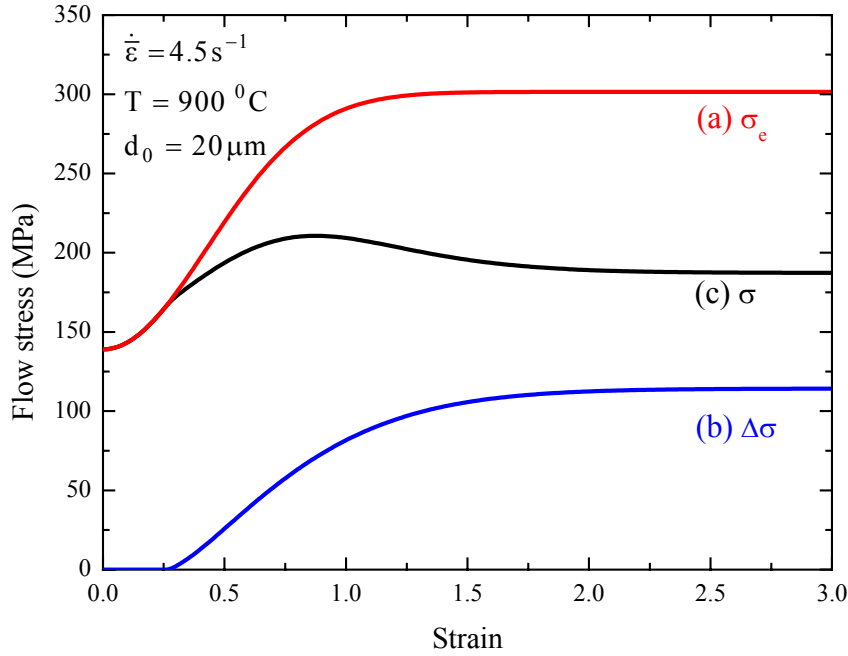where d_0 is the initial grain size whereas a, A, p and q are material parameters.

Figure 1: Flow-stress curve of low carbon steels. [9]

The softening due to the dynamic recrystallisation,[9] see curve (b) in Figure 1, is given by:

$$\Delta\sigma = (\sigma_{SS} - \sigma'_{SS}) \left\{ 1 - \exp\left[-k'\left(\frac{\bar{\varepsilon} - a\,\varepsilon_p}{\varepsilon_p} \right)^{m'} \right] \right\} \tag{15}$$

where σ'_{ss} is the current steady-state flow-stress at large strains whereas k' and m' are material parameters respectively. The curve (c) in Figure 1 is then obtained by superposing the effects of dynamic recovery and dynamic recrystallisation, namely, $\bar{\sigma} = \sigma_e$ if $\bar{\varepsilon} < \varepsilon_c$ and $\bar{\sigma} = \sigma_e - \Delta\sigma$ if $\bar{\varepsilon} \geq \varepsilon_c$.

It should be noted that for a general state of stress the effective strain $\bar{\varepsilon}$ must be calculated from the deformation strain-history. An appropriate procedure for obtaining

the effective strain is achieved from the material derivative in an Eulerian reference frame written in terms of the velocity field and its gradient as:

$$\dot{\overline{\varepsilon}} = \frac{D\overline{\varepsilon}}{Dt} = \frac{\partial \overline{\varepsilon}}{\partial t} + v \cdot \nabla \overline{\varepsilon} \tag{16}$$

where the term referring to the time derivative vanishes for a steady-state flow. Thus, Eq. (15) can be rewritten as a linear, hyperbolic differential equation with a source term to obtain the effective strain, that is, $\rho\dot{\overline{\varepsilon}} = \nabla \cdot (\rho v \overline{\varepsilon})$.

The stored energy resulting from the deformation of dislocations also promotes additional microstructure changes immediately after the unloading. These static restoration mechanisms can also be followed by grain growth if there is enough time between the deformation intervals, as is the case for plate and roughing mills. On the other hand, the hot strip or finishing process is characterized by decreasing time intervals and increasing strain-rates per pass and may, therefore, lead to dynamic recrystallisation followed by metadynamic recrystallisation. The latter starts from the partly or steadily recrystallised structure resulting from the dynamic recrystallisation after a deformation above the critical strain.[9] In order to take into account the partially recrystallised regions which may receive further deformation, the following correction for the effective strain is made:

$$\overline{\varepsilon} = \overline{\varepsilon}_N + (1 - X)\overline{\varepsilon}_{N-1} \tag{17}$$

where *N* is the current pass or stand and X is the static recrystallised volume fraction after the time *t* and is described by the JMKA model[10]:

$$X = 1 - \exp\left[-0.693\,(t/t_{0.5})^k\right] \tag{18}$$

where $t_{0.5}$ is the time needed for half recrystallisation. In plain C-Mn steels the exponent *k* is equal to 1.0 and 1.5 for static recrystallisation and metadynamic recrystallisation mechanisms respectively.[10]
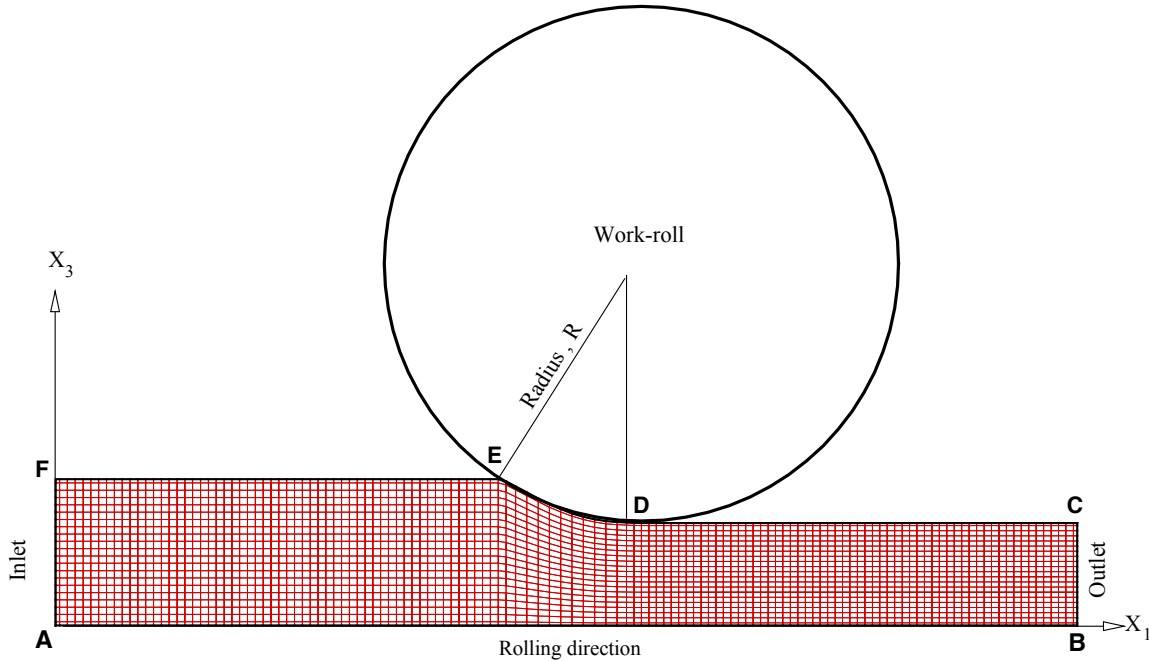
Figure 2: Finite volume mesh for a pass of the hot strip rolling process and imposed boundary conditions.

The corresponding C-Mn times for half recrystallisation and recrystallised grain sizes *d* for the recrystallisation events are predicted by the equations described in Sciliano et al.[10] Also, once recrystallisation is completed, the austenite grain may continue to growth as a function of the available time between the deformation intervals. This further grain growth dependence upon the time for the hot strip rolling of C-Mn steels is described by Sciliano et al.[10]

Figure 2 illustrates in a Cartesian coordinate system X_i (i = 1,2,3) the mesh used in the numerical simulations of the hot strip rolling. Due to the symmetry, only the half strip thickness is considered. The boundary conditions for momentum and heat transfer imposed at the boundary domain are regarded dependent upon the strand considered. The first strand assumes inlet velocity and fully developed flow at the outlet, which in turn, is the inlet velocity and temperature profiles for the next strand. At the free surfaces E-F and C-D, before and after the deformation zone, the dominant heat transfer mechanisms are convection and radiation. In the roll-gap, that is, at the contact region D-E between the strip and the work-roll, the heat transfer is mainly by conduction. At the symmetry plane A-B there is no heat flux along the direction X_3 as well as for the outlet section B-C along the normal direction X_1, see Fig. 2. The inlet temperature and the velocity field at the inlet section F-A for the first stand are assumed to be constant whereas the corresponding values at the outlet section B-C are computed from the transport equations.

3 RESULTS AND DISCUSSION

The calculations were carried out to a C-Mn steel with initial plate thickness equal to 35.4 mm with an average surface temperature of 984.7 ^{0}C and is reduced to 3.90 mm in a 7-stand finishing mill. The strip surface temperatures were measured with the help

of an optical pyrometer.[11] Table 1 shows the constitutive parameters describing the typical behaviour of C-Mn steels during hot strip rolling, Eqs. (16-21), which have been taken as the values available in the material database of the commercial code Slimmer.[5] The initial austenite grain size d_0 at the first stand was assumed to be equal to 120 μm. The apparent activation energy Q for the Zener-Hollomon parameter has set equal to 300 kJ/mol whereas the parameter C, see Eq.(13), is defined as:

$$C = 10\left[(\sigma_{01} - \sigma_0)/(\sigma_{SS} - \sigma_0) \right]^2 \tag{19}$$

Table1: Constitutive material data for C-Mn steels.[5]

	σ_0			σ_{SS}	
A_1	A_2	A_3	A_4	A_5	A_6
103.84	4.92×10^{13}	0.13	103.41	1.77×10^{11}	0.217
	σ_{01}			σ'_{SS}	
A_7	A_8	A_9	A_{10}	A_{11}	A_{12}
89.29	2.55×10^{11}	0.182	106.72	3.88×10^{12}	0.146
	$\Delta\sigma$			ε_p	
k'	m'	a	A	p	q
0.49	1.4	0.7	5.6×10^{-4}	0.3	0.17

Figure 3 shows the numerical predictions of flow stress and temperature distributions obtained for the first stand where a temperature increase is observed near to the strip central region up to the exit due to the conduction heat and generation from the plastic-work. In the roll bite region a strong variation of the flow stress is observed as consequence of high deformation rate and deformation. The flow stress increases to about 200 MPa due to the temperature decrease in the contact region with the work-roll.
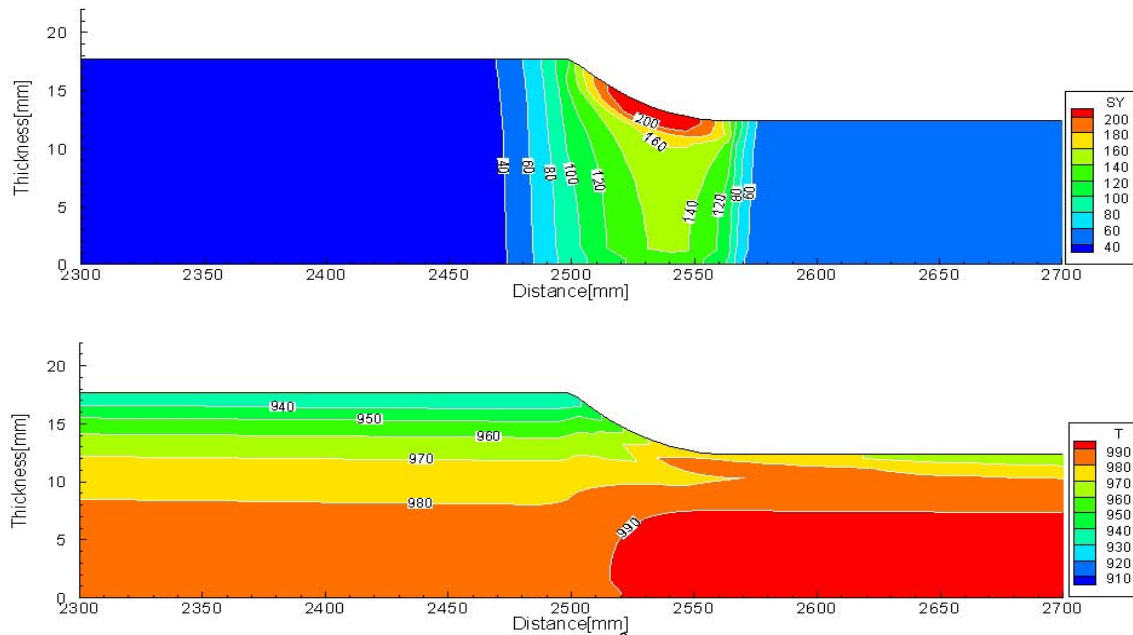

Figure 3: Predicted flow stress (MPa) and temperature (^{0}C) distributions obtained for the first stand of the hot rolling of a C-Mn steel strip

Table 2: Measured and predicted rolling loads.

Stand	F1	F2	F3	F4	F5	F6	F7
Measured (MN)	12.69	13.07	13.40	10.65	10.50	9.09	5.79
Predicted (MN)	12.68	13.09	13.40	10.56	10.38	9.08	5.68
Error (%)	0.07	0.15	0.00	0.84	1.10	0.11	1.89

Table 2 compares the numerical predictions with the measured rolling load data determined from the industrial rolling mill of a C-Mn steel strip. First of all, the FV model proposed in this work provides a very good prediction for the rolling loads. Secondly, since the deformation zone is strongly non uniform, as can be observed from Figure 3, the models which take into account uniform variables in this region, for instance, based upon Orowan's or Sim's works,[1,2] usually furnish poor predictions of the rolling loads.

On the other hand, Figure 4 compares the predicted temperature evolution with the interstand measured strip surface temperature. Strong variations of the temperature are observed during the hot strip rolling process. These variations strongly affect the materials properties and hence the rolling load prediction. Consequently, accurate computations of the local temperature are of fundamental importance for the description of the material flow stress and the prediction of material properties during the hot rolling process. Figure 5 shows the average austenite grain size evolution during the 7-stand finishing mill of a C-Mn. One can observe that the grain growth is stronger in the five first passes due to the longer interpass times and the temperature conditions. Moreover, the range of the predicted grain sizes are in agreement with the expected grain refinement during the hot strip rolling process and with the numerical results obtained by the model.
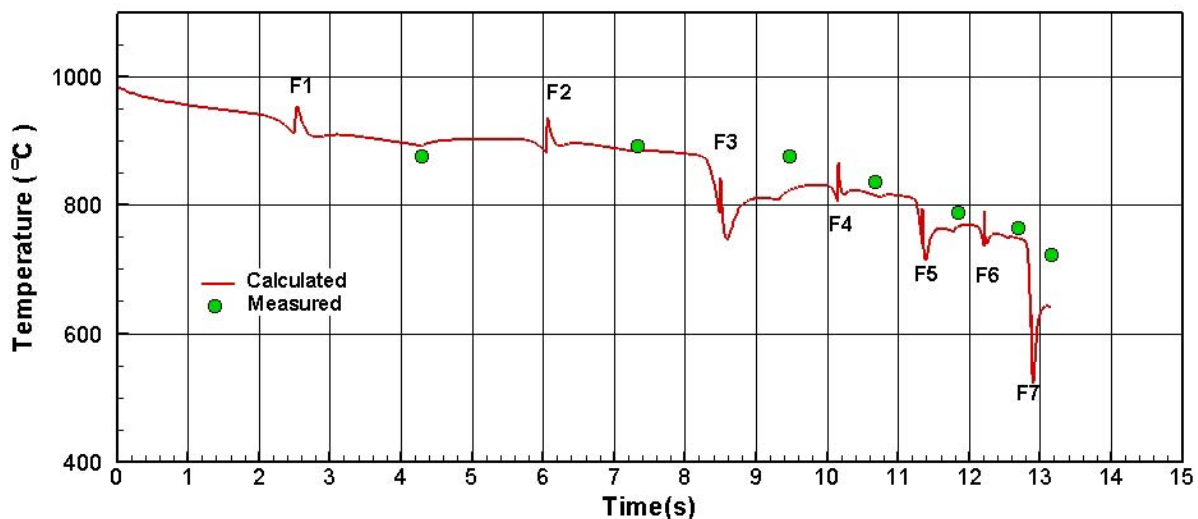

Figure 4: Predicted and measured temperature evolution during the hot strip rolling of C-Mn steel in a 7-stand finishing mill.
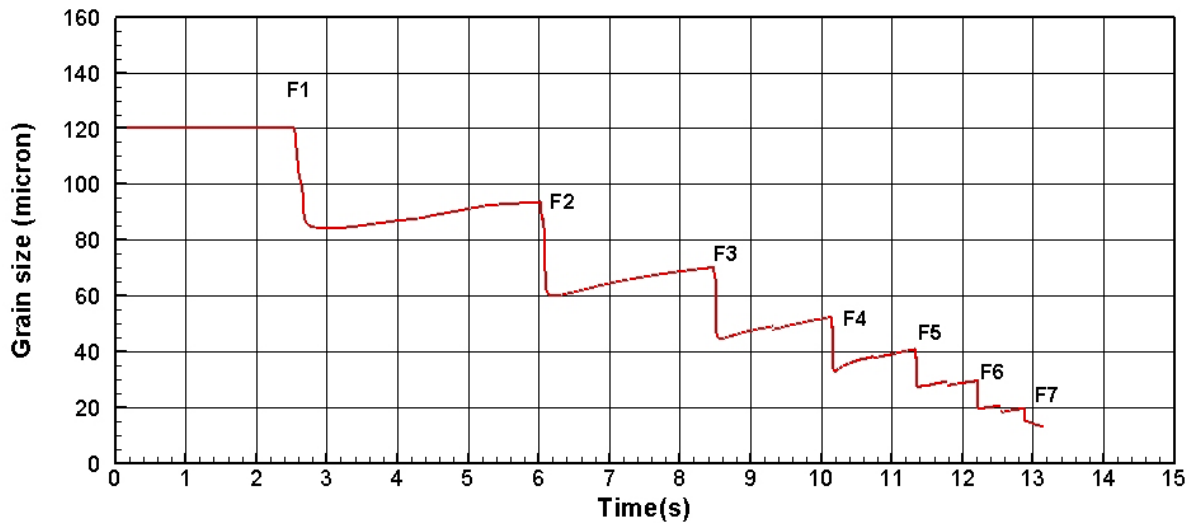
Figure 5: Predicted average austenite grain size evolution during the hot strip rolling of C-Mn steel in a 7-stand finishing mill.

4 CONCLUSIONS

In the present work, a finite volume based model has been developed which takes into account the heat transfer phenomena of the contact region and the combined convective and radiation heat transfer. The microstructural evolution during the hot deformation and interpass processes were also taken into consideration. A constitutive law for low C-Mn steels was used in a local frame in order to consider the simultaneous effects of temperature, strain rates, deformation and microstructural evolution. The predictions obtained for the temperature evolution and the rolling loads showed good agreement with the measured data from an industrial 7-stand hot strip finishing mill. Also, the predicted austenite grain size evolution indicates the typical grain refinement that can be achieved from the thermomechanical processing of low C-Mn steels.

Acknowlegements

REFERENCES

1 Orowan, E., The calculation of roll pressure in hot and cold flat rolling. *Proceedings of the Institution of Mechanical Engineers*, **150**, pp. 140-167, 1943.
2 Sims, E., The calculation of roll force and torque in hot rolling mills. *Proceedings of the Institution of Mechanical Engineers*, **168**, pp. 191-200, 1954.
3 Zhou, S. X., An integrated model for hot rolling of steel strips. *Journal of Materials Processing Technology*, **134(3)**, pp. 338-351, 2003.
4 Mukhopadhyay, A., Howard, I.C. and Sellars, C.M., Development and validation of a finite element model for hot rolling using ABAQUS/ STANDARD. *Materials Science and Technology*, **20(9)**, pp. 1123-1133, 2004.

5   SLIMMER, Sheffield Leicester Integrated Model for Microstructural Evolution in Rolling, Pro Technology, University of Leicester, Leicester, United of Kingdom, 1992.

6   Zienkiewicz, O.C., Jain, P.C. and Oñate, E., Flow of Solids During Forming and Extrusion : Some Aspects of Numerical Solutions. *International Journal of Solids and Structures*, **14(1)**, pp. 15-38, 1978.

7   Lenard, J.G., Pietrzyk, M. and Cser, L., *Mathematical and Physical Simulation of the Properties of Hot Rolled Products*, Elsevier: Oxford and New York, pp. 105-150, 1999.

8   Thompson, J. F., Warsi, Z. U. A. and Mastin, C.W., Numerical Grid Generation. North Holland: New York, Appendix C-3, p. 454, 1985.

9   Beynon, J. H. and Sellars, C. M., Modelling microstructure and its effects during multipass hot rolling, *The Iron and Steel Institute of Japan*, **32(3)**, pp. 359-367, 1992.

10 Siciliano Jr., F., Minami, K., Maccagno, T. M. and Jonas, J. J., Mathematical Modeling of the Mean Flow Stress, Fractional Softening and Grain Size During the Hot Strip Rolling of C-Mn Steels. *The Iron and Steel Institute of Japan*, **36(12)**, pp. 1500-1506, 1996.

11 Radespiel, E. S., Silva, A. J., Reick, W. and Silva, M.A.C., Mathematical modelling and numerical simulation of thermomechanical and microstructural evolution of steels during hot-rolling, THERMEC'97, ed. T. Chandra, TMS, pp. 217-223, 1997.